*Environ. Sci. Technol.* **1998**, *32,* 1771−1778

# Snow Scavenging of Polychlorinated Biphenyls and Polycyclic Aromatic Hydrocarbons in Minnesota

THOMAS P. FRANZ AND
STEVEN J. EISENREICH*

*Department of Environmental Sciences, 14 College Farm Road, Rutgers University, New Brunswick, New Jersey 08901*

Snow and rain events were collected with concurrent air samples during the winter of 1991−1992 at a suburban site in Minnesota to investigate atmospheric scavenging of polychlorinated biphenyls (PCBs) and polycyclic aromatic hydrocarbons (PAHs). Particle scavenging was the dominant contributor to the total concentrations in snow and was less important in rain. Gas scavenging was only important for low molecular weight PCB congeners and PAHs. Enrichment of dissolved-phase concentrations over levels predicted from temperature-corrected Henry's Law constants was observed for low molecular weight compounds in both rain and snow. The particulate fraction ($\phi$) of atmospheric PCBs and PAHs was the best indicator of total scavenging ($W_T$) by snow according to the equations log $W_T = 0.71$ ($\pm$0.08) log $\phi + 5.34$ ($\pm$0.08) for PCB congeners ($r = 0.62$) and log $W_T = 0.89$ ($\pm$0.12) log $\phi + 6.07$ ($\pm$0.13) for PAHs ($r = 0.73$).

## Introduction

The process by which atmospheric organic compounds are preferentially removed from the atmosphere in cold regions has been termed "global distillation" (*1*), "cold trap condensation" (*2*−*4*), and "global fractionation and cold condensation" (*5*). Cold-temperature removal of organic chemicals results from the reduction of vapor pressure with temperature, which consequently enhances gas/particle and gas/ice partitioning. Although a significant proportion of annual precipitation occurs as snow in northern latitudes, little is known about the scavenging of atmospheric organic contaminants by snow.

Most of the available literature regarding the interactions between snow and atmospheric contaminants pertains to inorganic chemicals. The purpose of this manuscript is to document the scavenging of atmospheric semivolatile organic chemicals (SOCs) by snow. Gas and particle scavenging coefficients are calculated for PCBs and PAHs in three individual snow events and one winter rain event. Scavenging from dry snowfalls typical in colder, Arctic regions is discussed elsewhere (*6*).

**Snow Scavenging.** In mixed-phase clouds, ice crystals grow at the expense of liquid droplets due to differences in the vapor pressure of water over the liquid and ice surfaces. Thus, droplet concentrations increase while diluting those of ice crystals growing by vapor diffusion (the Bergeron−Findeisen process) (*7*−*10*). Large settling crystals can intercept cloud droplets (>10 $\mu$m) as they sweep through the cloud, an accretion process known as riming (*9, 11*). Since cloud droplets contain most of the aerosol mass within the cloud, riming can yield concentrations in precipitation that are similar to cloud droplet concentrations (*8, 9, 12, 13*). Rimed snows are thus more efficient at accumulating atmospheric contaminants and contain higher concentrations than unrimed snow events formed by diffusional growth (*7*−*9, 14, 15*).

Hydrometeors exiting the cloud base intercept additional particles and gases enroute to the surface. In precipitation occurring during unstable atmospheric conditions, below-cloud scavenging is less important than in-cloud scavenging (*16*−*19*). However, when stable atmospheric stratification causes contaminants to accumulate within the surface boundary layer, below-cloud scavenging may contribute significantly to wet deposition (*20*).

Scavenging of atmospheric gases and particles is described by (*21*)

$$W_T = W_g(1 - \phi) + W_p(\phi) \quad (1)$$

where $W_T$, $W_g$, and $W_p$ are the dimensionless total, gas, and particle scavenging ratios, respectively, and $\phi$ is the fraction of the total atmospheric concentration associated with particulate matter. Then, $W_g = C_{S,d}/C_{A,g}$, and $W_p = C_{S,p}/C_{A,p}$, where $C_{S,d}$ and $C_{S,p}$ are the snow concentrations (ng/m$^3$) of the SOC in the dissolved and particle phases, respectively, and $C_{A,g}$ and $C_{A,p}$ are the air concentrations (ng/m$^3$) in the gas and particle phases.

Differences in scavenging between rain and snow occur because of the dissimilarities in the physical state of the hydrometeor, liquid versus solid. Theoretically, a trace gas attaining equilibrium with a cloud droplet or raindrop is scavenged by dissolution according to Henry's Law:

$$W_g = RT/K_H = \alpha \quad (2)$$

where $R$ is the universal gas constant ($8.21 \times 10^{-5}$ atm m$^3$/mol K), $T$ is temperature (K), $K_H$ is Henry's Law constant (atm m$^3$/mol) corrected to ambient temperature, and $\alpha$ is the theoretical gas scavenging ratio or the reciprocal dimensionless Henry's Law constant. For snow, this equation may not apply since only a thin liquid water film exists on the surface of ice crystals. At temperatures <1 °C and in the absence of ions, the film may be less than 5 nm thick, whereas impurities within the water layer may cause the film to thicken to 30 nm at −15 °C (*22*−*24*). Thus, gas scavenging by snow may be better described as vapor sorption to a liquid interface (*25*−*27*)

$$W_{g,ads} = K_{ia}SA_s\rho \quad (3)$$

where $K_{ia}$ is the interfacial adsorption coefficient (m) defined as the ratio of the mass adsorbed per surface area of sorbent (i.e., snow) (ng/m$^2$) to the atmospheric vapor phase concentration (ng/m$^3$), $SA_s$ is the specific surface area (m$^2$/g), and $\rho$ is density of ice (0.917 g/cm$^3$). Recently, Pankow (*28*) reported $K_{ia}$ values for PAHs and *n*-alkanes, although $K_{ia}$ values for PCBs remain unknown. Similarly, the specific surface area of snow is uncertain and depends on crystalline shape, but is thought to range from <0.1 to >1.0 m$^2$/g (*26*).

In rimed snow, both dissolution and adsorption mechanisms may apply with interfacial adsorption occurring to the surface water film and with Henry's Law dissolution into

* Corresponding author fax: 732-932-8644; e-mail: eisenreich@aesop.rutgers.edu.

S0013-936X(97)00601-9 CCC: $15.00 
Published on Web 05/12/1998

cloud droplets scavenged by snowflakes falling through the cloud. Because scavenged droplets freeze upon contact with the snowflake, Henry's Law partitioning behavior may only be observed if there is negligible loss of contaminants during freezing of the droplets (*29*−*32*).

Organic surface films on snow crystals may also enhance gas adsorption. Such films are likely to be discontinuous, i.e., less than one monolayer thick. About 200 mg/L of surface-active organic matter is necessary for monolayer coverage of a 6 mm diameter platelike crystal (*33*). Nevertheless, the presence of any organic film can potentially enhance adsorption of SOCs to snow.

Snow may be more efficient than rain at below-cloud scavenging of particles because of the larger size and surface area of snowflakes (*8*, *17*, *19*, *34*−*38*). The particle scavenging efficiency of snow is related to crystalline shape with needles and columns less effective than stellar plates, dendrites, and snowflakes (*39*, *40*). Snowflakes and dendritic crystals exhibit a "filtering effect" on atmospheric particles enroute to the surface due to their porosity, which allows air to pass through the falling solid. This ventilation enhances the ability of snowflakes and dendrites to scavenge small particles (0.2−2 $\mu$m), which tend to follow the streamlines around a nonporous raindrop (*34*, *41*). Field experiments have demonstrated that below-cloud scavenging of particles by snow is about five times more efficient than by rain (*17*, *42*).

## Experimental Section

**Sampling Protocol.** Four precipitation events were collected concurrently with air samples during the winter of 1991−1992 approximately 30 km west of Minneapolis/St. Paul, MN (44°57′N, 93°39′W). Since fresh snowfall can be characterized as a loose collection of individual crystals or ice grains, snow events could be distinguished from the compact, cohesive structure of the underlying snowpack. The snow event was collected by scraping or sweeping the fresh snow from the snowpack surface with an aluminum shovel and storing the snow in 110 L aluminum containers covered with a foil-lined aluminum lid. Subsamples were also collected for dissolved organic carbon (DOC) and suspended particulate matter (SPM).

A manual rain collector (1 $m^2$ aluminum surface) was employed to capture rain. The lid was removed just prior to the onset of rain and water was isolated within a sealed 20 L stainless steel canister. Immediately after the event, the surface of the collector was flushed with Milli-Q water (Millipore), and collected with the rainwater. A manual wipe of the surface was considered unnecessary since particles were likely to be loosely associated with the still wet surface. In the laboratory, the canister was pressurized with nitrogen forcing the water through a 90 mm diameter glass fiber filter (GFF) and a Teflon cartridge (15 cm × 1.5 cm i.d.) containing cleaned Amberlite XAD-2 resin (Sigma Chemical Co.).

Air samples were taken concurrently with the precipitation events using Graseby General Metal Works (Cleves, OH) high-volume samplers. Air was passed through a GFF (Schleicher and Schuell, No. 25, 20 × 25 cm) and a polyurethane foam (PUF) plug (8 cm diameter × 10 cm height, 0.049 g/$cm^3$ density) at a rate of 0.5−1.2 $m^3$/min (face velocities of 17−40 cm/s). Two samplers were operated simultaneously to obtain a sufficient mass of particulate material, one with the configuration described above, the other with a filter only.

The snow was thawed for 2−5 days at 4 °C. The snowmelt was maintained at 4 °C and was filtered through 293 mm diameter GFFs. The filtrate, collected in precleaned 65 L stainless steel tanks, was passed through an XAD-2 resin column (glass cartridge, 2.5 cm i.d. × 20 cm) at flow rates of 100−200 mL/min. The snow cans were rinsed with 2 L of Milli-Q water and filtered with the remaining sample. This method allowed for the determination of both dissolved (XAD-2) and particulate (GFF) fractions within the snowmelt.

The snow subsamples were transferred to 2 L glass beakers and allowed to thaw at room temperature while covered with aluminum foil. Approximately 250−750 mL of the meltwater was filtered through a 0.4 $\mu$m Nuclepore filter for suspended particulate matter (SPM) analysis. The remainder was filtered through 47 mm glass fiber filters and collected in polyethylene bottles for DOC analysis.

**Analytical Procedure.** The analytical procedure consisted of sequential 24 h Soxhlet extractions of the XAD resin and snow GFFs using methanol and dichloromethane. Air samples were Soxhlet extracted for 24 h using dichloromethane (GFFs) or 20% (v/v) dichloromethane in petroleum ether (PUFs). Analytical details are similar to descriptions in Achman et al. (*43*) and Hornbuckle et al. (*44*). The concentrated extracts were analyzed on either an HP-5890 GC with $^{63}$Ni electron capture detector (PCBs) or an HP-5890 GC with an HP-5970 mass selective detector (PAHs) using DB-5 glass capillary columns (J&W Scientific).

Nuclepore filters (SPM) were dried overnight at 50 °C and placed in a desiccator prior to weighing on a Perkin-Elmer model AD-2 microbalance. Dissolved organic carbon (DOC) was measured following combustion at 750 °C on an Ionics Model 555 Total Organic Carbon Analyzer.

**Quality Control/Quality Assurance.** Details of the various quality control parameters monitored during this study are described elsewhere (*45*). Briefly, surrogate recoveries were 105 ± 16% for PCB congener #166 (2,3,4,4′,5,6-hexachlorobiphenyl) and 89 ± 10% for $d_{12}$-chrysene. Detection limits ranged from 0.001 to 0.04 ng for PCB congeners (0.7 ng for Σ-PCBs) and from 0.01 to 0.1 ng for individual PAHs. PCB congener levels in matrix blanks ranged from 0.004 to 2.3 ng, while Σ-PCBs ranged from a low of 2.8 ± 1.3 ng in air GFFs to a high of 17 ± 13 ng in PUFs. For individual PAHs, matrix blank levels ranged from 0.02 to 8 ng and were quite consistent among all matrices. All samples were blank corrected. Results reported as "Σ-PCBs" represent the summed contribution of 57 chromatographic PCB congener peaks representing 87 individual or coeluting congeners, while "Σ-PAHs" is the sum of 17 individual PAHs.

To simulate a field snow blank, a snow canister was filled with Milli-Q water and subjected to the filtration and XAD isolation procedure. The mass from 39 L through an XAD column ranged from 0.01 to 2.6 ng for PCB congeners and 19 ng for Σ-PCBs, representing a concentration of 0.50 ng/L. For individual PAHs, the mass ranged from 0.3 to 94 ng (0.01−2.4 ng/L). The corresponding filter through which 62 L flowed contained 0.01−0.27 ng for PCB congeners and 2.1 ng for Σ-PCBs (0.03 ng/L), and from 0.6 to 3.8 ng for individual PAHs (0.01−0.06 ng/L).

Two half PUF plugs in series were used to evaluate breakthrough of gas-phase PCBs and PAHs. The mass of Σ-PCBs on the secondary PUF averaged 18 ± 10% ($n$ = 9) of the total mass (primary plus backup PUF) with air volumes of 418−668 $m^3$ at average surface temperatures between 4 and −6 °C. Σ-PAHs behaved similarly with secondary PUF masses averaging 12 ± 3% ($n$ = 9) of the total mass. Thus, greater than 90% of gas-phase compounds were quantitatively retained by the PUFs under the conditions encountered.

Backup GFFs were employed with three air samples to evaluate gas-phase adsorption to the filter. For Σ-PCBs, adsorption onto the secondary (2°) GFF accounted for an average 13 ± 6% ($n$ = 3) of the primary (1°) filter mass. Adsorption of Σ-PAHs to the 2° GFF averaged 3.0 ± 4.4% ($n$ = 3) and was dominated by lower molecular weight PAHs with mean adsorption ranging from 5 to 18% of the 1° GFF mass. These results are in agreement with Ligocki and Pankow (*46*), who found that adsorption to the 2° GFF was highly variable with averages ranging from 4 to 29%.

**TABLE 1. Meteorological Conditions during Winter Precipitation Events**

| sample | date | times[a] | av surface temp (°C) | type of precipitation | total precipitation (mm) | snow depth (cm) | time | cloud[b] base (m) | av cloud temp (°C) |
|---|---|---|---|---|---|---|---|---|---|
| air 1 | 12/11−12/91 | 13:00−01:00 | −1.0 ± 1.3 | | | | | | |
| air 2 | 12/12/91 | 01:00−15:00 | 1.0 ± 1.1 | | | | | | |
| rain | 12/12/91 | 04:30−11:30 | 1.0 ± 0.6 | light rain, freezing rain, fog | 12.4 | | 11:00 on 12/12/91 | 1000 | −2.0 ± 2.5 |
| air 3 | 12/12−13/91 | 11:30−01:30 | −0.9 ± 3.2 | | | | | | |
| air 4 | 12/13/91 | 01:00−14:00 | −5.4 ± 3.1 | | | | | | |
| snow | 12/13/91 | 14:00−19:45 | 1.3 ± 0.6 | light snow | 1.3 | 0.7 | 11:30 on 12/13/91 | 1300 | −10.5 ± 5.3 |
| | 12/14/91 | 03:30−07:45 | −11.0 ± 1.0 | light snow | | | 12:15 on 12/14/91 | 600 | −17.9 ± 3.8 |
| air 5 | 12/13−14/91 | 14:00−08:00 | −4.6 ± 4.9 | | | | | | |
| air 6 | 12/19/91 | 11:00−23:00 | −3.7 ± 2.0 | | | | | | |
| snow | 12/19−20/91 | 17:45−04:30 | −1.8 ± 0.7 | light snow, ice pellets, freezing rain, graupel | 4.1 | 0.7 | 11:30 on 12/19/91 | 2500 | −5.9 ± 1.4 |
| | | | | | | | 11:00 on 12/20/91 | 0 | −2.1 ± 0.8 |
| air 7 | 12/19−20/91 | 21:00−12:00 | −0.9 ± 1.0 | | | | | | |
| air 8 | 3/8−9/92 | 12:30−02:30 | 4.4 ± 2.7 | | | | | | |
| | | | | | | | 11:15 on 3/8/92 | 400 | 0.1 ± 1.3 |
| snow | 3/8−9/92 | 19:30−07:45 | 0.3 ± 3.1 | light rain, snow | 17 | 6 | 11:00 on 3/9/92 | 2100 | −10.5 ± 3.1 |

[a] Time period of air sample and precipitation. [b] Cloud conditions determined from radiosonde observations at St. Cloud, MN, approximately 100 km northwest of GFBI. Altitude of cloud base is estimated from relative humidity profile.

Volatilization of SOCs from filtered particles was negligible because of the low ambient temperatures (*47*).

## Results and Discussion

**Precipitation Events.** Four precipitation events (Table 1) were obtained during the winter of 1991−1992. Precipitation took a variety of forms including freezing rain, sleet/ice pellets, and graupel, in addition to rain and snow. The snowfall (~1 cm) on December 13−14, 1991, had a density of 0.19 g/cm$^3$, typical of relatively "wet" snow events occurring at surface temperatures near 0 °C. "Dry" snowfalls that occur at subzero conditions have densities of ~0.05−0.1 g/cm$^3$. The December 19−20 snowfall (~1 cm) was a mixture of snow, sleet, graupel, and freezing rain with a high density of 0.58 g/cm$^3$. The March 8−9, 1992, event (~6 cm) could be characterized as a heavy, wet snow as indicated by its 0.28 g/cm$^3$ density. Although no attempt was made to characterize the snow crystal types or the extent of riming occurring during these events, rimed snow did contribute to the December 19−20 snowfall since graupel is an extreme form of riming.

Average surface temperatures during the events ranged from +1 to −11 °C, while average cloud temperatures were estimated to range from −2 to −18 °C (Table 1). Radiosonde profiles of the atmosphere were obtained at noon at a site ~100 km northwest of the sampling site (*48*). The temperature and relative humidity profiles were interpreted to estimate the altitude of cloud base and average temperature within the clouds. Because the radiosonde data are not closely linked in time with the onset of precipitation or with the location of the sampling site, the cloud conditions in Table 1 are only indicative of regional atmospheric conditions.

Atmospheric concentrations of SOCs associated with each event are listed in Table 2, while concentrations in precipitation are listed in Table 3. The rain event that began during the morning of Dec 12 was associated with a low-pressure center moving east. As southwest surface winds shifted to the east prior to the onset of precipitation, air concentrations of Σ-PCBs rose from ~350 to 550 pg/m$^3$ and Σ-PAHs increased from ~15 to 24 ng/m$^3$. As average temperatures rose from −1.0 to +1.0 °C, the atmospheric particle fraction of Σ-PCBs remained nearly constant at ~10% of the total concentration, and particulate Σ-PAHs fell from 17 to 11% of the total concentration. The concentrations of Σ-PCBs and Σ-PAHs in the rain were 2.8 and 81 ng/L, respectively, with particle washout accounting for 66% of the Σ-PCBs and 40% of the Σ-PAHs in the rain. Scavenging of atmospheric gases accounted for >50% of the total concentration of di- and trichlorobiphenyls and PAHs with molecular weights < pyrene (202 amu). Particle-scavenging ratios of the rain ranged from about $10^3$ to $10^5$ for both PCBs and PAHs.

Following the rain event, air sampling continued as a fast-moving cold front, an "Alberta Clipper", moved out of Canada. Air concentrations of Σ-PCBs decreased to 80 pg/m$^3$ and Σ-PAHs diminished to 12 ng/m$^3$ during the day of Dec 13. Snow occurred the evening of Dec 13 and again the morning of Dec 14. The initial snowfall, which accounted for most of the accumulation, occurred as the front approached. Nighttime gas-phase concentrations of SOCs during the snowfall were less than the day before. Although no filter data are available during the snow event, atmospheric particulate SOC levels likely decreased also.

High concentrations of both Σ-PCBs (7.9 ng/L) and Σ-PAHs (18 μg/L) were detected in the snow. As illustrated in Figure 1, snow concentrations were much higher than in the rain event and occurred as atmospheric SOC levels plummeted over the previous 36 h. Higher SOC concentrations in snow than in rain have been reported (*37*, *49*−*53*). This behavior has been attributed to the enhanced particle-scavenging efficiency of snow (*37*) and to reduced atmospheric mixing heights and photodegradation rates during the winter (*50*). Particle scavenging accounted for 88% of Σ-PCBs and 94% of Σ-PAHs in the snow with $W_P$ values of $3 \times 10^5$ to $5 \times 10^7$.

The suspended particulate matter (SPM) concentration of the snow (225 mg/L) was more than 2 orders of magnitude higher than that in the rain (1.1 mg/L), while dissolved organic carbon (DOC) concentrations were similar (Table 3). This supports the contention that snow is more efficient than rain at scavenging atmospheric particles. Average monthly TSP levels ranged from 30 to 110 μg/m$^3$ in the Minneapolis/St. Paul metropolitan area during the winter of 1991−1992 (*54*). From SPM in the precipitation events and average winter TSP levels, $W_P$ for TSP is estimated to be ~$10^4$ for the Dec 12 rain and ~$5 \times 10^6$ for the Dec 14 snowfall, in general agreement with the SOC results.

Following passage of the cold front on Dec 14, subzero temperatures persisted in the upper Midwest. On Dec 19, a low-pressure front moved across the central plains and temperatures rose from −17 to −3 °C as winds shifted to the

**TABLE 2. Air Concentrations (pg/m³) of PCBs and PAHs during the Winter of 1991−1992[a]**

| chemical | air 1 12/11−12/91 before rain | air 2 12/12/91 during rain | air 3[b] 12/12−13/91 after rain | air 4 12/13/91 before snow | air 5[b] 12/13−14/91 during snow | air 6 12/19/91 before/during snow | air 7[b] 12/19−20/91 during/after snow | air 8 3/8−9/92 before/during snow |
|---|---|---|---|---|---|---|---|---|
| PCB homologues | | | | | | | | |
| dichlorobiphenyls | 38.7 (37) | 57.8 (13) | 18.9 | 23.1 (0.3) | 10.8 | 37.7 (3) | 71.3 | 23.1 (2) |
| trichlorobiphenyls | 72.3 (9) | 160.8 (3) | 51.3 | 21.5 (4) | 15.2 | 60.3 (5) | 60.9 | 36.5 (2) |
| tetrachlorobiphenyls | 98.7 (3) | 142.6 (6) | 32.6 | 16.2 (4) | 9.1 | 27.7 (21) | 26.5 | 21.8 (7) |
| pentachlorobiphenyls | 54.0 (3) | 64.1 (9) | 12.0 | 9.9 (12) | 5.0 | 12.9 (20) | 8.6 | 16.2 (8) |
| hexachlorobiphenyls | 27.5 (7) | 40.7 (26) | 7.9 | 6.6 (15) | 3.3 | 4.8 (37) | 2.2 | 12.1 (7) |
| heptachlorobiphenyls | 43.9 (8) | 62.3 (13) | 1.5 | 4.7 (70) | 0.5 | 3.6 (86) | 0.7 | 11.7 (24) |
| octachlorobiphenyls | 12.0 (12) | 20.0 (11) | 0.2 | 0.4 (82) | 0.1 | 1.5 (99) | 0.1 | 4.4 (38) |
| total PCBs | 347 (9.5) | 548 (8.5) | 124 | 82 (8.9) | 44 | 149 (15) | 170 | 126 (7.3) |
| PAHs | | | | | | | | |
| acenaphthylene | 2620 (0.1) | 4250 (0.1) | 1690 | 2020 (0.3) | 398 | 1460 (0.3) | 570 | 335 (1) |
| acenaphthene | 693 (0.4) | 1080 (0.3) | 596 | 668 (0.5) | 230 | 466 (2) | 302 | 276 (1) |
| fluorene | 2200 (0.5) | 4565 (0.2) | 1750 | 1810 (0.8) | 549 | 1450 (1) | 1010 | 1170 (1) |
| phenanthrene | 4340 (3) | 7950 (1.5) | 3635 | 3350 (3) | 1255 | 3250 (7) | 1900 | 2770 (4) |
| anthracene | 312 (3) | 469 (2) | 240 | 210 (5) | 82 | 183 (11) | 84 | 129 (9) |
| fluoranthene | 1320 (18) | 1875 (10) | 840 | 987 (19) | 315 | 1310 (33) | 625 | 862 (21) |
| pyrene | 1080 (18) | 1465 (11) | 702 | 849 (19) | 259 | 875 (36) | 370 | 613 (21) |
| retene | 82 (33) | 134 (14) | 65 | 131 (27) | 15 | 118 (25) | 42 | 157 (8) |
| benz[*a*]anthracene | 138 (89) | 129 (81) | 6 | 92 (96) | 3 | 127 (98) | 4 | 73 (90) |
| chrysene | 345 (89) | 341 (80) | 27 | 266 (91) | 11 | 370 (95) | 32 | 148 (80) |
| benzo(b+k)fluoranthene | 558 (97) | 536 (98) | 1 | 413 (100) | ND | 570 (99) | 5 | 236 (98) |
| benzo[*e*]pyrene | 232 (98) | 254 (99) | ND[c] | 178 (100) | ND | 226 (99) | 4 | 104 (98) |
| benzo[*a*]pyrene | 126 (96) | 117 (100) | ND | 92 (100) | ND | 130 (98) | ND | 65 (100) |
| indeno(c,d)pyrene | 233 (98) | 258 (99) | ND | 174 (100) | ND | 211 (99) | ND | 99 (100) |
| dibenz(a,h)anthracene | 32 (92) | 30 (100) | ND | 23 (100) | ND | 32 (95) | ND | 18 (100) |
| benzo(g,h,i)perylene | 311 (98) | 431 (>99) | ND | 245 (100) | ND | 232 (99) | ND | 104 (100) |
| total PAHs (ng/m³) | 14.6 (17) | 23.9 (11) | 9.6 | 11.5 (17) | 3.1 | 11.0 (26) | 5.0 | 7.2 (18) |

[a] Total concentration is sum of vapor and particulate phases. The particulate percentage is shown in parentheses. [b] Vapor phase only. [c] Not detected (ND).

**TABLE 3. Concentrations of PCBs (pg/L) and PAHs (ng/L) in Winter 1991−1992 Precipitation[a]**

| chemical | rain 12/12/91 | snow 12/13−14/91 | snow 12/19−20/91 | snow 3/8−9/92 |
|---|---|---|---|---|
| PCB homologues (pg/L) | | | | |
| dichlorobiphenyls | 385 (18) | 672 (40) | 134 (49) | 94 (25) |
| trichlorobiphenyls | 236 (11) | 1370 (82) | 1080 (61) | 490 (68) |
| tetrachlorobiphenyls | 841 (74) | 1920 (94) | 1210 (86) | 534 (83) |
| pentachlorobiphenyls | 983 (84) | 1130 (93) | 710 (86) | 246 (83) |
| hexachlorobiphenyls | 217 (95) | 1180 (96) | 602 (95) | 191 (90) |
| heptachlorobiphenyls | 76 (56) | 1140 (94) | 651 (94) | 260 (94) |
| octachlorobiphenyls | 40 (80) | 498 (99) | 204 (98) | 98 (>99) |
| total PCBs | 2780 (66) | 7910 (88) | 4590 (82) | 1910 (79) |
| PAHs (ng/L) | | | | |
| acenaphthylene | 2.3 (3) | 5 (74) | 2.1 (73) | 0.5 (79) |
| acenaphthene | 1.2 (9) | 211 (80) | 27 (84) | 3 (68) |
| fluorene | 5.6 (4) | 364 (78) | 44 (82) | 4 (75) |
| phenanthrene | 24.5 (13) | 3590 (85) | 515 (82) | 57 (86) |
| anthracene | 0.7 (47) | 300 (92) | 43 (94) | 5 (95) |
| fluoranthene | 13.7 (38) | 1890 (88) | 677 (91) | 82 (93) |
| pyrene | 13.9 (45) | 3115 (95) | 491 (93) | 60 (95) |
| retene | 1.4 (55) | 50 (96) | 7 (94) | 1.4 (98) |
| benz[*a*]anthracene | 1.3 (92) | 976 (99) | 65 (97) | 22 (99) |
| chrysene | 3.7 (84) | 1420 (98) | 211 (96) | 32 (97) |
| benzo[*b*+*k*]fluoranthene | 4 (>99) | 2085 (>99) | 499 (>99) | 84 (>99) |
| benzo[*e*]pyrene | 2.1 (93) | 873 (>99) | 210 (>99) | 36 (>99) |
| benzo[*a*]pyrene | 2.9 (98) | 905 (>99) | 179 (>99) | 37 (>99) |
| indeno[*c*,*d*]pyrene | 1.3 (100) | 871 (>99) | 169 (>99) | 26 (>99) |
| dibenz[*a*,*h*]anthracene | 0.4 (100) | 186 (>99) | 32 (100) | 4.5 (100) |
| benzo[*g*,*h*,*i*]perylene | 1.7 (100) | 736 (>99) | 145 (>99) | 22 (>99) |
| total PAHs (ng/L) | 81 (40) | 17580 (94) | 3320 (93) | 477 (96) |
| SPM (mg/L) | 1.1 | 225 ± 10 | 20.6 ± 0.8 | 4.0 ± 1.3 |
| DOC (mg C/L) | 13.0 ± 1.0 | 11.8 ± 0.8 | 4.5 ± 1.2 | 18.4 ± 1.5 |

[a] Total concentration is sum of dissolved and particulate phases, the particulate percentage of the total is shown in parentheses.

south. Snow, sleet, and graupel began the evening of Dec 19. Atmospheric levels of Σ-PCBs were nearly constant during the frontal passage with concentrations of ~160 pg/m³ (15% particulate), while Σ-PAHs diminished from 11 to ~5 ng/m³ (26% particulate) (Table 2). The snowfall had a Σ-PCB concentration of 4.6 ng/L and a Σ-PAH concentration

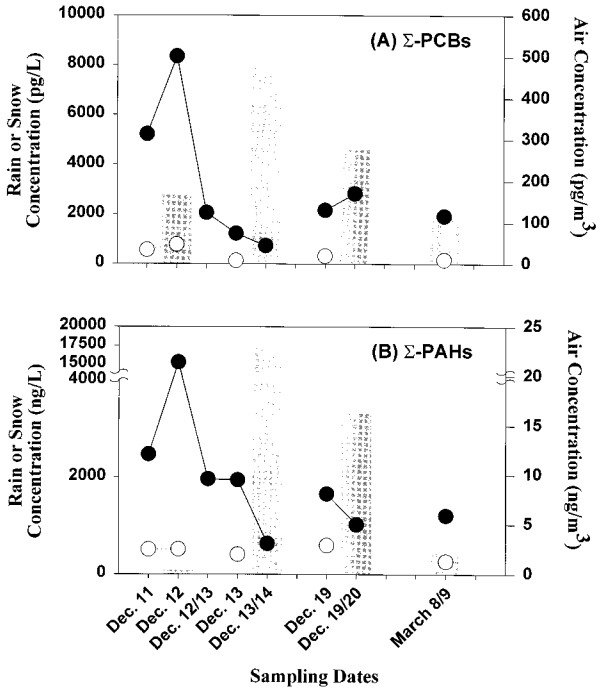


**FIGURE 1. Concentrations of (A) ∑-PCBs and (B) ∑-PAHs in precipitation events during the winter of 1991−1992. Bars represent total (dissolved plus particulate) rain or snow concentrations, while the solid (●) and open (○) circles are the atmospheric gas and particle concentrations, respectively.**

of 3.3 $\mu$g/L (Table 3). Particle washout accounted for 82% of the ∑-PCB content of the snow and 93% of ∑-PAHs, similar to the Dec 14 snow event.

Although atmospheric levels of PAHs during the Dec 19−20 snow were similar to the levels encountered by the Dec 14 snow and accumulations of ~1 cm were associated with both events, the ∑-PAH concentrations on Dec 20 were nearly five times less than the snow of Dec 14. Particle scavenging during the Dec 19−20 snow may have been less effective because a portion of the precipitation occurred as freezing rain and sleet. Values of $W_P$ ranged from $5 \times 10^4$ to $2 \times 10^6$ during this mixed event. These scavenging ratios are generally an order of magnitude less than the $W_P$ values determined for the Dec 14 snowfall, suggesting that freezing rain/sleet may be less efficient than snow in scavenging atmospheric particles. This is supported by the SPM concentration of 21 mg/L, which is an order of magnitude less than in the Dec 14 snowfall (225 mg/L).

On March 7, a slight drizzle occurred on the leading edge of a cold front. As the front passed on March 8, winds shifted to the north and light rain turned to snow as temperatures cooled during the evening. By the morning of March 9, temperatures had fallen to −5 °C and ~6 cm of snow had accumulated. The air concentration of ∑-PCBs was 126 pg/m$^3$ (7% particulate), and the ∑-PAH concentration was ~7 ng/m$^3$ (18% particulate) from a sample taken just prior to and during the snowfall. The snow had a ∑-PCB concentration of 1.9 ng/L and a ∑-PAH concentration of 0.5 $\mu$g/L, which are less than the levels detected in the December snow events. Since the initial stages of the event began as rain and were not sampled, the snow concentrations may not reflect the scavenging that occurred throughout the entire event. Particulate SOC scavenging ratios ranged from $5 \times 10^4$ to $6 \times 10^5$. However, the rain may have washed out a fraction of the atmospheric particles determined by the air sample, such that the snow encountered an atmosphere reduced in particulate SOCs. The resulting snow $W_P$ values may therefore be underestimated.

**Gas Scavenging.** Previous studies have suggested that gas-scavenging ratios of SOCs by rain are near equilibrium as predicted by temperature-corrected $K_H$ values (*21*, *55*) or are supersaturated because of the presence of nonfilterable colloidal material in the filtrate (*53*, *56*, *57*). Here, measured gas-scavenging ratios ($W_g$) are compared to theoretical gas scavenging ratios $\alpha$, calculated from temperature-corrected Henry's Law constants ($K_H$) according to eq 2. This approach assumes that gaseous SOCs dissolve into the surface water film of the snow crystals or cloud droplets scavenged by rimed snow. Operationally, dissolved compounds are those determined in the meltwater following filtration. Whether these chemicals were incorporated within the crystalline lattice, truly dissolved in the surface film or cloud droplets captured by riming, or adsorbed to the solid crystal or liquid surface film is unknown.

Potential artifacts include volatilization from the snow canister as melting proceeds, inclusion of colloids in the dissolved fraction, and desorption/adsorption within meltwaters. Volatilization losses were minimized by maintaining the meltwater at 4 °C. The inclusion of colloidal material in the dissolved phase would suggest that the truly dissolved phase is less than observed. Desorption kinetics are fast for <50% of particle bound SOCs (*58*). Desorption/adsorption artifacts are minimized by maintaining the snowmelt temperature at 4 °C and filtering as soon as possible after thawing (*59*). A comparison of the dissolved/particle distribution coefficient ($K_d$) as a function of the octanol−water partition coefficient ($K_{ow}$) between snow events and snowpacks that suffered some melting in the field revealed differences ($p < 0.05$) in their log $K_d$ versus log $K_{ow}$ relationships (*45*). In contrast, significant similarities ($p < 0.05$) were found between snow events and snowpacks not exposed to melting. This ability to observe differences in the dissolved/particle distributions among various snow samples using the same analytical protocols suggests that desorption/adsorption artifacts in the meltwater are small.

Subcooled liquid $K_H$ values at 25 °C (*60*, *61*) were corrected to ambient temperature using the equation

$$\log K_{H(T)} = \log K_{H(298)} + \frac{\Delta H_W}{2.3R(298)} - \frac{\Delta H_W}{2.3RT} \qquad (4)$$

where $R$ is the ideal gas constant (8.314 J/mol K) and $\Delta H_W$ is the enthalpy of vaporization from water. The average enthalpy of vaporization (~65 kJ/mol) from Tateya et al. (*62*) was used to represent all PCB congeners. Ten Hulscher et al. (*63*) measured $\Delta H_W$ values of <52 kJ/mol for three low molecular weight PCB congeners and reported literature values that ranged from 50 to 65 kJ/mol for PCB congeners containing up to six congeners. A difference of only ~0.2 log units in log $K_H$ at 0 °C results when $\Delta H_W$ values of 52 or 65 kJ/mol are used in eq 4. For individual PAHs, $K_H$ constants (*61*) were temperature corrected using $\Delta H_W$ values of 26 to 82 kJ/mol (*63*, *64*).

Analysis of the four precipitation events revealed that there was no correlation ($p > 0.05$) between measured log $W_g$ and calculated log $\alpha$ for PCB congeners. For PAHs, all snow events exhibited strong correlations ($r = 0.70-0.91$, $p < 0.05$) between log $W_g$ and log $\alpha$, while there was little correlation ($r = 0.41$) in the rain event. Thus, gas-phase PAHs demonstrated dissolution behavior unlike PCBs in snow. A mechanistic explanation for the different gas-scavenging behavior between these two classes of SOCs is problematic. One possible reason is that the temperature correction applied to $K_H$ for PCBs assumes that all congeners behave similarly, i.e., that the enthalpy of volatilization from water is the same for each PCB congener. This may be an oversimplification as suggested by the individual effect of temperature on $K_H$ among the PAHs.

Another possibility is that interfacial adsorption of gaseous PCBs and PAHs occurred to the liquid water film on the snow surface rather than dissolution as predicted by $K_H$. Valsaraj et al. (*27*) demonstrated that enrichment of gas-phase SOCs in fog, greater than predicted by Henry's Law, could be explained by adsorption to the air−water interface. Enrichment factors ($E$) are defined as the ratio of the measured gas scavenging ratio ($W_g$) to the theoretical value ($\alpha$):

$$E = W_g/\alpha \quad (5)$$

Enrichment ($E > 1$) increases with a chemical's hydrophobicity and decreases with increasing size of water drops (*27*, *65*). Thus, dissolution accounts for the chemical mass incorporated into large rain drops, while surface adsorption is important for small cloud and fog droplets because the available surface can "hold" more chemical mass than can dissolve into the bulk water. For snow, interfacial adsorption should dominate gas scavenging since only a thin water film exists on the surface.

Enrichment factors ($E$) for each precipitation event were calculated from measured $W_g$ values and temperature-corrected $\alpha$ values. Contrary to predictions (*27*), $E$ generally decreased with increasing molecular weight for both PCBs and PAHs with the lower molecular weight species enriched ($E > 1$), while high molecular weight SOCs had $E$ values <1. Rain $E$ values were relatively close to equilibrium with geometric means of 0.5 for PCBs and 0.14 for PAHs. Poster and Baker (*56*) reported mean enrichments of about 100 for both PCBs and PAHs in rain that was attributed to nonfilterable colloidal material in the filtrate. Here, unsaturated conditions suggest that colloids were not important in this rain event. Geometric mean $E$ values among the snow events ranged from 0.75 to 2.2 for PCBs and from 0.43 to 20 for PAHs. In the March snow event (geometric means $E = 0.4-0.75$), gas scavenging was near equilibrium with $K_H$ predictions. In the December snow events, either colloids or interfacial adsorption contributed to elevated dissolved concentrations.

To further investigate interfacial adsorption, theoretical-scavenging ratios ($W_{g,ads}$) were calculated using eq 3 and the relationship for PAHs (*28*):

$$\log K_{ia} = -1.2 \log p_L^\circ - 5.82 \quad (6)$$

Subcooled liquid vapor pressures ($p_L^\circ$) at 25 °C for PAHs (*61*) were corrected to ambient temperatures according to correlations by Hinckley et al. (*66*) or by extrapolation of data in Eisenreich and Strachan (*67*). A specific surface area ($SA_s$) of 0.1 $m^2/g$ (*68*) for snow resulted in theoretical gas scavenging ratios due to interfacial adsorption ranging from $\sim 10^3$ to $10^{10}$. All snow events exhibited strong correlations ($r = 0.77-0.95$, $p < 0.05$) between log $W_g$ and log $W_{g,ads}$, although slopes were significantly <1 ($m = 0.20-0.31$). The correlations between measured $W_g$ and theoretical-scavenging ratios due to interfacial adsorption were stronger than those based on dissolution among the snow events and were weaker than dissolution correlations in the rain event. Thus, interfacial adsorption may have occurred in the snow events.

In summary, gas scavenging by snow could not be explained by either Henry's Law dissolution or interfacial adsorption for PCBs, although PAHs did exhibit dissolution and adsorption behavior. It is suspected that destruction of the crystalline structure by melting alters the dissolved/particle distribution originally present in the snow. Quantifying the extent of this alteration will require a nondestructive analytical technique that maintains the integrity of the crystalline snow structure. Nevertheless, gas scavenging by snow was a minor contributor to the deposition of PCBs and PAHs accounting for <20% of Σ-PCBs and <10% of Σ-PAHs.

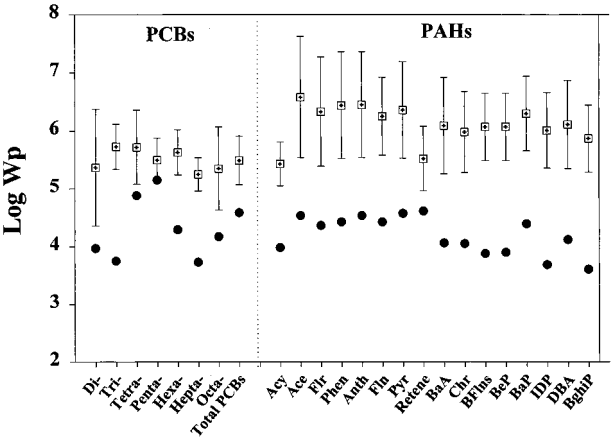


**FIGURE 2. Calculated particle scavenging ratios ($W_P$) for PCB homologues and PAHs in winter rain (●) and snow events (□, mean ± one standard deviation).**

**Particle Scavenging.** Particle-scavenging ratios for SOCs are shown in Figure 2 and range from $10^3$ to $10^5$ for winter rain and from $5 \times 10^4$ to $5 \times 10^7$ for the snow events. The snow was an order of magnitude more efficient than rain at scavenging particulate matter from the atmosphere. In the winter rain event, 66% of the total Σ-PCB concentration and 40% of the total Σ-PAH concentration was associated with particulate matter. The particle contribution to the snow accounted for 80−88% of Σ-PCBs and 93−96% of Σ-PAHs. Thus, particle-scavenging dominates atmospheric deposition by snow, although a significant amount of low molecular weight gaseous SOCs are incorporated into both rain and snow.

Close agreement is noted between $W_P$ values in the literature and those determined in this study (*6*) for organic chemicals having similar atmospheric particle size distributions, i.e., mass median diameters <1.0 $\mu$m (*69*). Published particle scavenging ratios for elemental carbon, POC, PAHs, *n*-alkanes, PCBs, dioxins, and furans range from $10^2$ to $10^6$ for rain (*51*, *52*, *55*, *57*, *70*−*75*) and from $10^4$ to $10^6$ for snow (*51*, *76*). The high $W_P$ of $>10^7$ for a few PAHs during one snow event suggests that atmospheric conditions may occasionally be favorable for very efficient particle scavenging. Such situations may result from significant below-cloud scavenging during snow events of low intensity occurring near emission sources. Alternatively, ground level air concentrations during this event may have been less than within the precipitating cloud.

Since the fraction of the total atmospheric concentration of SOCs associated with particulate matter ($\phi$) is a function of $P_L^\circ$ (*77*−*80*), a relationship between $p_L^\circ$ and $W_p$ might be expected. Conversely, since the capture efficiency of particles by hydrometeors is strongly dependent on particle size (*81*), $W_p$ may be independent of $\phi$ and $p_L^\circ$. Then, $W_p$ may be more indicative of the size distribution of atmospheric particles than the partitioning behavior of SOCs. For exchangeable SOCs that partition between various particle sizes, such as the more volatile, lower molecular weight PAHs (*82*), $W_p$ will be higher for those SOCs that are associated with large particles (*55*, *57*, *70*).

Correlations between log $W_p$ and log $p_L^\circ$ for both PCBs and PAHs were not significant ($p > 0.05$) in the snow events. This suggests that $W_p$ is generally invariant and primarily depends on the size distribution of atmospheric particles (*70*). Conversely, significant correlations ($p < 0.05$) between log $W_p$ and log $p_L^\circ$ were found for PCBs and PAHs in the rain

event. Although the slopes were <0.2, particle scavenging increased with $p_L^\circ$. The more volatile, lower molecular weight SOCs may have been associated with larger particles that were scavenged more efficiently.

Similar behavior was indicated by the relationship between log $W_p$ and log $\phi$ for these winter precipitation events. Particle scavenging ratios for snow were either invariant or decreased as $\phi$ increased. Thus, particle scavenging was slightly greater for the more volatile PCBs and PAHs. This suggests that lower molecular weight SOCs are associated with a different particle size spectrum than their less volatile counterparts.

The significant correlations ($p < 0.05$) between log $W_p$ and log $\phi$ for both PCBs and PAHs in the rain event support this observation. The slight negative slopes (>−0.36) indicate that particle scavenging by rain is less efficient for high molecular weight SOCs that are predominantly associated with submicron atmospheric particles. Similarly, Poster and Baker (*57*) found that particle-scavenging ratios in rain were higher for PAHs associated with particles (>0.5 $\mu$m) than for those associated with submicron particles (<0.5 $\mu$m).

**Total Scavenging.** From a modeling perspective, it is more important to assess the total scavenging ($W_T$) of an atmospheric contaminant from some measurable air parameter or chemical property than the individual contribution from gas or particle scavenging. For example, eq 1 illustrates that $W_T$ is highly dependent on the particulate fraction ($\phi$) of SOCs in the atmosphere. Therefore, if $\phi$ can be measured or predicted, then $W_T$ may be estimated. Similarly, since $\phi$ is related to vapor pressure (*77*−*80*), it may be possible to estimate $W_T$ from $p_L^\circ$. Correlations between $W_T$ and $\phi$ were evaluated for the winter precipitation events to determine if relationships existed which could be utilized for modeling atmospheric deposition.

In the rain event, $W_T$ ranged from $\sim 10^3$ to $10^5$ for PCB congeners and from $5 \times 10^2$ to $2.5 \times 10^4$ for PAHs. Regressions between log $W_T$ and log $\phi$ revealed no significant correlation ($p > 0.05$) between these parameters for PCBs. However, a relationship was noted for PAHs (log $W_T = 0.37 \log \phi + 4.0$, $r = 0.87$, $p < 0.05$).

Among the snow events, $W_T$ ranged from $\sim 10^3$ to $10^7$ for PCBs and PAHs. Significant correlations ($p < 0.05$) were found between log $W_T$ and log $\phi$ for both PCBs ($r = 0.54-0.68$) and PAHs ($r = 0.85-0.97$) with scavenging increasing with increasing $\phi$. Since there was no difference in the regression slopes among the snow events, regressions were performed on the entire snow data set. The resulting regressions are (Figure 3)

$$\text{PCBs: } \log W_T = 0.71\ (\pm 0.08) \log \phi + 5.34\ (\pm 0.08) \quad (r = 0.62,\ p < 0.05) \quad (7)$$

$$\text{PAHs: } \log W_T = 0.89\ (\pm 0.12) \log \phi + 6.07\ (\pm 0.13) \quad (r = 0.73,\ p < 0.05) \quad (8)$$

The slope for PCBs is significantly different from both zero and unity, while the PAH slope is not different from 1. For comparison, the regression for the winter rain event is also shown in Figure 3. Snow is a more effective scavenger of SOCs than rain if the SOCs have an appreciable atmospheric particle fraction (i.e., >1−5%).

Because particle scavenging by rain and snow dominants wet deposition, the influence of temperature on gas/particle partitioning and the predominance of snow during the winter in high latitudes enhances the removal of organic chemicals from the atmosphere. Snow is much more effective at scavenging atmospheric particles than rain because of its porosity. Current sampling techniques limit our ability to determine the importance of interfacial adsorption.

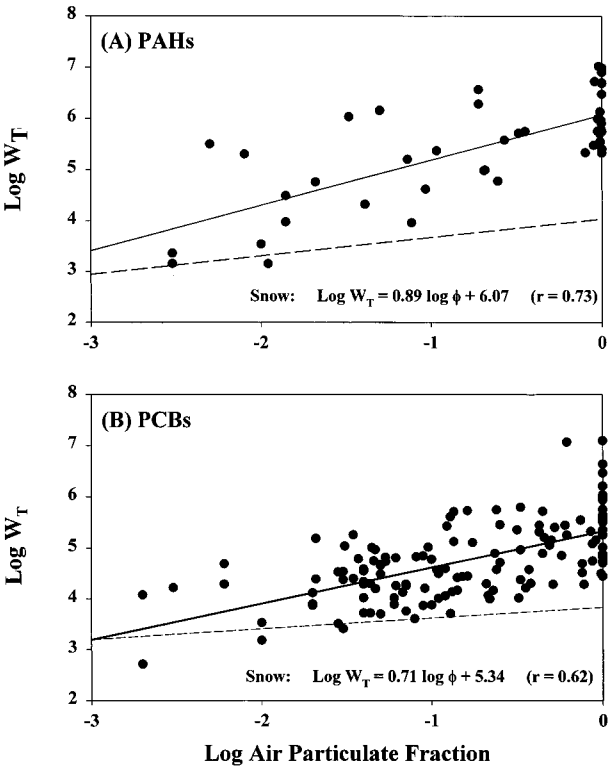


**FIGURE 3. Correlations between total scavenging ratios ($W_T$) and the air particulate fraction of (A) PAHs and (B) PCB congeners in snow events (●, solid line is linear regression). For comparison, the linear regression of the winter rain event is also shown (dashed line).**

## Acknowledgments

The authors wish to thank Brian Soltis for his care and patience in assisting with the laboratory analysis of the air and precipitation samples. This work was funded by the Great Lakes Protection Fund, Grant FG6901029 and by the U.S. Environmental Protection Agency, Grant EPA/R995233-01-0, D. Anderson, Project Officer.

## Literature Cited

(1) Goldberg, E. D. *Proc. R. Soc. London, Ser. B*, **1975**, *189*, 277.
(2) Ottar, B. *Atmos. Environ.* **1981**, *15*, 1439.
(3) Rahn, K. A.; Heidam, N. *Atmos. Environ.* **1981**, *15*, 1345.
(4) Weschler, C. J. *Atmos. Environ.* **1981**, *15*, 1365.
(5) Wania, F.; Mackay, D. *Ambio* **1993**, *22*, 10.
(6) Franz, T. P.; Gregor, D. J.; Eisenreich, S. J. In *Atmospheric Deposition of Contaminants to the Great Lakes and Coastal Waters*; Baker, J. E., Ed.; SETAC Press: New York, 1997; pp 73−107.
(7) Scott, B. C. *J. Appl. Met.* **1981**, *20*, 619.
(8) Parungo, F.; Nagamoto, C.; Madel, R. *J. Atmos. Sci.* **1987**, *44*, 3162.
(9) Borys, R. D.; Hindman, E. E.; DeMott, P. J. *J. Atmos. Chem.* **1988**, *7*, 213.
(10) Collett, J. L. Jr.; Oberholzer, B.; Mosimann, L.; Staehelin, J.; Waldvogel, A. *Water Air Soil Pollut.* **1993**, *68*, 43.
(11) Pruppacher, H. R. In *Clouds: Their Formation, Optical Properties, and Effects;* Hobbs, P. V., Deepak, A., Eds.; Academic Press: New York, 1981; pp 93−186.
(12) Barrie, L. A. *J. Geophys. Res.* **1985**, *90*D, 5789.
(13) Collett, J. L. Jr.; Oberholzer, B.; Staehelin, J. *Atmos. Environ.* **1993**, *27*A, 33.
(14) Mitchell, D. L.; Lamb, D. *J. Geophys. Res.* **1989**, *94*D, *14*, 831.
(15) Collett, J. L. Jr.; Prevot, A. S. H.; Steahelin, J.; Waldvogel, A. *Environ. Sci. Technol.* **1991**, *25*, 782.
(16) Scott, B. C. In *Atmospheric Pollutants in Natural Waters*; Eisenreich, S. J., Ed.; Ann Arbor Sciences: Ann Arbor, MI, 1981; pp 3−21.
(17) Murakami, M.; Kimura, T.; Magono, C.; Kikuchi, K. *J. Met. Soc. Jpn.* **1983**, *61*, 346.

(18) Rehkopf, J.; Newiger, M.; Grassl, H. *Atmos. Environ*. **1984**, *18*, 2745.
(19) Schumann, T.; Zinder, B.; Waldvogel, A. *Atmos. Environ*. **1988**, *22*, 1443.
(20) Zinder, B.; Schumann, T.; Waldvogel, A. *Atmos. Environ*. **1988**, *22*, 2741.
(21) Ligocki, M. P.; Leuenberger, C.; Pankow, J. F. *Atmos. Environ*. **1985**, *19*, 1609.
(22) Kvlividze, V. I.; Kiselev, V. F.; Kurzaev, A. B.; Ushakova, L. A. *Surface Sci*. **1974**, *44*, 60.
(23) Beaglehole, D.; Nason, D. *Surface Sci*. **1980**, *96*, 357.
(24) Valdez, M. P.; Dawson, G. A.; Bales, R. C. *J. Geophys. Res*. **1989**, *94*D, 1095.
(25) Goss, K.-U. *Environ. Sci. Technol*. **1993**, *27*, 2826.
(26) Hoff, J. T.; Wania, F.; Mackay, D.; Gillham, R. *Environ. Sci. Technol*. **1995**, *29*, 1982.
(27) Valsaraj, K. T.; Thoma, G. J.; Reible, D. D.; Thiboduex, L. J. *Atmos. Environ*. **1993**, *27*A, 203.
(28) Pankow, J. F. *Atmos. Environ*. **1997**, *31*, 927.
(29) Uhlmann, D. R.; Chalmers, B.; Jackson, K. A. *J. Appl. Phys*. **1964**, *35*, 2986.
(30) Hoekstra, P.; Miller, R. D. *J. Colloid Interface Sci*. **1967**, *25*, 166.
(31) Gross, G. W.; Wu, C.-H.; Bryant, L.; McKee, C. *J. Chem. Phys*. **1975**, *62*, 3085.
(32) Lamb, D.; Blumenstein, R. *Atmos. Environ*. **1987**, *21*, 1765.
(33) Gill, P. S.; Graedel, T. E.; Weschler, C. J. *Rev. Geophys. Space Phys*. **1983**, *21*, 903.
(34) Redkin, Yu. N. In *Hydrodynamics and Thermodynamics of Aerosols*; Voloshchuk, V. M.; Sedunov, Yu. S., Eds.; John Wiley and Sons: New York, 1973; pp 226−238.
(35) Graedel, T. E.; Franey, J. P. *Geophys. Res. Lett*. **1975**, *2*, 325.
(36) Raynor, G. S.; Hayes, J. V. In *Precipitation Scavenging, Dry Deposition, and Resuspension*; Pruppacher, H. R.; Semonin, R. G.; Slinn, W. G. N., Eds.; Elsevier Science Publishing: New York, NY, 1983; pp 249−264.
(37) Leuenberger, C.; Czuczwa, J.; Heyerdahl, E.; Giger, W. *Atmos. Environ*. **1988**, *22*, 695.
(38) Nicholson, K. W.; Branson, J. R.; Giess, P. *Atmos. Environ*. **1991**, *25*A, 771.
(39) Takahashi, T. *J. Met. Soc. Jpn*. **1963**, *41*, 327.
(40) Miller, N. L.; Wang, P. K. *Atmos. Environ*. **1991**, *25*A, 2593.
(41) Mitra, S. K.; Barth, U.; Pruppacher, H. R. *Atmos. Environ*. **1990**, *24*A, 1247.
(42) Sparmacher, H.; Fülber, K.; Bonka, H. *Atmos. Environ*. **1993**, *27*A, 605.
(43) Achman, D. R.; Hornbuckle, K. C.; Eisenreich, S. J. *Environ. Sci. Technol*. **1993**, *27*, 75.
(44) Hornbuckle, K. C.; Achman, D. R.; Eisenreich, S. J. *Environ. Sci. Technol*. **1993**, *27*, 87.
(45) Franz, T. P. Ph.D. Dissertation, University of Minnesota, Minneapolis, MN, 1994.
(46) Ligocki, M. P.; Pankow, J. F. *Environ. Sci. Technol*. **1989**, *23*, 75.
(47) Zhang, X.; McMurry, P. H. *Environ. Sci. Technol*. **1991**, *25*, 456.
(48) National Climactic Data Center, National Weather Service, Asheville, NC, 1992.
(49) Meyers, P. A.; Hites, R. A. *Atmos. Environ*. **1982**, *16*, 2169.
(50) Czuczwa, J.; Leuenberger, C.; Giger, W. *Atmos. Environ*. **1988**, *22*, 907.
(51) McVeety, B. D.; Hites, R. A. *Atmos. Environ*. **1988**, *22*, 511.
(52) Swackhamer, D. L.; McVeety, B. M.; Hites, R. A. *Environ. Sci. Technol*. **1988**, *22*, 664.
(53) Murray, M. W.; Andren, A. W. *Atmos. Environ*. **1992**, *26*A, 883.
(54) Minnesota Pollution Control Agency, Air Quality Division, St. Paul, MN, 1992.
(55) Dickhut, R. M.; Gustafson, K. E. *Environ. Sci. Technol*. **1995**, *29*, 1518.
(56) Poster, D. L.; Baker, J. E. *Environ. Sci. Technol*. **1996**, *30*, 341.
(57) Poster, D. L.; Baker, J. E. *Environ. Sci. Technol*. **1996**, *30*, 349.
(58) Pignatello, J. J.; Xing, B. *Environ. Sci. Technol*. **1996**, *30*, 1−11.
(59) Jickells, T. D.; Davis, T. D.; Tranter, M.; Landsberger, S.; Jarvis, K.; Abrahams, P. *Atmos. Environ*. **1992**, *26*A, 393.
(60) Brunner, S.; Hornung, E.; Santi, H.; Wolff, E.; Piringer, O. G.; Altschuh, J.; Brüggemann, R. *Environ. Sci. Technol*. **1990**, *24*, 1751.
(61) Mackay, D.; Shiu, W. Y.; Ma, K. C. *Illustrated Handbook of Physical-Chemical Properties and Environmental Fate for Organic Chemicals;* Lewis Publishers: Ann Arbor, MI, 1992.
(62) Tateya, S.; Tanabe, S.; Tatsukawa, R. In *Toxic Contamination in Large Lakes*; Schmidtke, N. W., Ed.; Lewis Publishers: Chelsea, MI, 1988; Vol. III, pp 237−281.
(63) Ten Hulscher, Th. E. M.; Van der Velde, L. E.; Bruggeman, W. A. *Environ. Toxicol. Chem*. **1992**, *11*, 1595.
(64) Eisenreich, S. J. Rutgers University, New Brunswick, NJ, unpublished results.
(65) Hoff, J. T.; Mackay, D.; Gillham, R.; Shiu, W. Y. *Environ. Sci. Technol*. **1993**, *27*, 2174.
(66) Hinckley, D. A.; Bidleman, T. F.; Foreman, W. T. *J. Chem. Eng. Data* **1990**, *35*, 232.
(67) Eisenreich, S. J.; Strachan, W. M. J. *Estimating Atmospheric Deposition of Toxic Substances to the Great Lakes*; International Joint Commission Report: Burlington, ON, 1992.
(68) Hoff, J. T.; Gregor, D.; Mackay, D.; Wania, F.; Jia, C. Q. *Environ. Sci. Technol*. **1998**, *32*, 58.
(69) Bidleman, T. F. *Environ. Sci. Technol*. **1988**, *22*, 361 (Errata: *22*, 726).
(70) Ligocki, M. P.; Leuenberger, C.; Pankow, J. F. *Atmos. Environ*. **1985**, *19*, 1619.
(71) Eitzer, B. D.; Hites, R. A. *Environ. Sci. Technol*. **1989**, *23*, 1396.
(72) Koester, C. J.; Hites, R. A. *Environ. Sci. Technol*. **1992**, *26*, 1375.
(73) Farmer, C. T.; Wade, T. L. *Water Air Soil Pollut*. **1986**, *29*, 439.
(74) Atlas, E.; Giam, C. S. *Water Air Soil Pollut*. **1988**, *38*, 19.
(75) Duinker, J. C.; Bouchertall, F. *Environ. Sci. Technol*. **1989**, *23*, 57.
(76) Cadle, S. H.; Dasch, J. M. *Atmos. Environ*. **1988**, *22*, 1373.
(77) Junge, C. E. In *Fate of Pollutants in the Air and Water Environments*; Suffett, I. H., Ed.; John Wiley & Sons: New York, 1977; pp 7−26.
(78) Bidleman, T. F.; Billings, W. N.; Foreman, W. T. *Environ. Sci. Technol*. **1986**, *20*, 1038.
(79) Pankow, J. F. *Atmos. Environ*. **1987**, *21*, 2275.
(80) Foreman, W. T.; Bidleman, T. F. *Atmos. Environ*. **1990**, *24*A, 2405.
(81) Slinn, W. G. N. In *Air-Sea Exchange of Gases and Particles*; Liss, P. S.; Slinn, W. G. N., Eds.; D. Reidel Publishing: Boston, MA, 1983; pp 299−405.
(82) Pistikopoulos, P.; Wortham, H. M.; Gomes, L.; Masclet-Beyne, S.; Bon Nguyen, E.; Masclet, P. A.; Mouvier, G. *Atmos. Environ*. **1990**, *24*A, 2573.

*Received for review July 3, 1997. Revised manuscript received January 26, 1998. Accepted March 19, 1998.*

ES970601Z